SUPPORTING INFORMATION

The growth of sodic amphibole at the greenschist- to blueschist-facies transition (Dent Blanche, Western Alps): bulk-rock chemical control and thermodynamic modelling

Paola Manzotti [12*], Michel Ballèvre [3], Pavel Pitra [3 4], Benita Putlitz [2], Martin Robyr [2], Othmar Müntener [2]

Affiliations:

[1] Department of Geological Sciences, Stockholm University, 106 91 Stockholm, Sweden

[2] Institute of Earth Sciences, University of Lausanne, Géopolis, Quartier Mouline, 1015 Lausanne, Switzerland

[3] Univ Rennes, CNRS, Géosciences Rennes - UMR 6118, F-35000 Rennes, France

[4] Česká geologická služba, Prague 1, Czech Republic

*Correspondence: paola.manzotti@geo.su.se , Tel. +46 (0)8 16 4745, ORCID: 0000-0002-6945-9878

Reference	Location	Rock type / paragenesis	Mineral	Chemical analyses	Whole rock analysis	Inferred metamorphic facies conditions
Diehl (1938), Stutz (1940)	Ollomont	hornblendite	gl		X	
Diehl et al. (1952)	Alpe Berrio	q-ab-Na am			X	
Hunziker (1974)	Southern side of Mt Gelé (KAW 943) ? - Ollomont (Alpe Berrio) (KAW 750) ?	q-pl-gl				
Ayrton et al. (1982)	Mont Dolin (Arolla Series)	paragneiss, prasinite, calcaires spathiques	am, blue at the core, green at the rim			
Ballèvre & Kienast (1987)	Becca di Salé	metachert	blue am			
De Leo et al. (1987)		mylonitic orthogneiss	blue am, aeg			
Canepa et al. (1990)			Fe-gl	X		blueschist or glaucophane-bearing greenschist-facies
Pennacchioni & Guermani (1993)		Arolla orthogneiss	aeg-aug, gl			D1 relatively high P D2-D3 greenschist facies
Roda & Zucali (2008, 2011)	Mont Morion	metagranite	mrbk, Fe-wnc	X		blueschist facies
Manzotti (2011)	Roisan-Cignana Shear Zone	metachert				blueschist facies
Manzotti et al. (2012)	Becca di Salé, Cuney	metachert	mrbk, wnc	X		blueschist facies
Baletti et al. (2012)	Sassa	mesocratic meta-gabbro	mrbk, wnc			blueschist facies
Manzotti et al. (2014a)	Roisan-Cignana Shear Zone	orthogneiss	mrbk, wnc	X		blueschist facies
Angiboust et al. (2014)	Mont Dolin , Pas de Chèvres	Arolla gneiss	mrbk, wnc	X		blueschist facies
Dal Piaz et al. (2015)	Arpisson lake, Blavy		Fe±gl			blueschist facies

TABLE S1 Occurrences of sodic amphibole and/or sodic pyroxene in the DBTS.

Mineral symbols used in this study

ab	albite
acm	acmite
act	actinolite
aeg	aegirine
aln	allanite
alm	almandine
am	amphibole
ap	apatite
aug	augite
bi	biotite
cal	calcite
chl	chlorite
cor	corundum
ctd	chloritoid
cu	cummingtonite
ep	epidote
g	garnet
gl	glaucophane
gr	grossular
hem	hematite
hb	hornblende
ilm	ilmenite
kfs	K-feldspar
jd	jadeite
ky	kyanite
law	lawsonite
mnz	monazite
mrbk	Mg-riebeckite
mt	magnetite
mu	muscovite
o	ompachite
ol	olivine
pa	paragonite
pl	plagioclase
prg	pargasite
pump	pumpellyite
q	quartz
ru	rutile
spss	spessartine
sph	titanite
srp	serpentine
st	staurolite
tr	tremolite
xtm	xenotime
wnc	winchite
zrn	zircon

Other symbols (mole/atomic proportions)

X_{Fe}	$Fe^{2+} / (Fe^{2+} + Mg)$	for amp,
X_{Fe3}	$Fe^{3+} / (Fe^{3+} + Al)$	for amp
Xps	$Fe^{3+} / (Fe^{3+} + Al^{3+})$	for ep
Mg#	(molar Mg / $(Mg+Fe^{2+})$	
alm	Fe/(Fe + Mg + Ca + Mn)	
py	Mg/(Fe + Mg + Ca + Mn)	
gr	Ca/(Fe + Mg + Ca + Mn)	
spss	Mn/(Fe + Mg + Ca + Mn)	
X_{Na}	Na / (Na + Ca)	amp
a.p.f.u.	per formula unit	
wt%	weight per cent	
mol.%	mole per cent	
vol. %	volume per cent	

TABLE S2: Mineral and other symbols used in this study.

	Na amphibole		Na-Ca amphibole		Ca amphibole						Chlorite		Epidote	
	OL02 mrbk	OL02 mrbk	OL02 wnc	OL02 wnc	OL02 act	OL02 act	OL02 Mg-hb	OL02 prg	OL02 prg	OL02 edn	OL02 chl	OL02 chl	OL02 ep core (matrix)	OL02 ep rim (matrix)
SiO_2	54.75	54.82	55.68	55.12	52.54	54.14	50.66	44.24	43.76	45.61	29.26	29.48	38.43	37.71
TiO_2	0.03	0.01	0.02	0.03	0.02	0.00	0.62	0.95	1.42	1.13	0.04	0.07	0.00	0.04
$Al2O_3$	3.95	3.28	1.84	1.52	2.89	1.47	5.82	13.24	12.61	10.50	17.02	16.88	27.09	22.04
Fe_2O_3*	24.49	22.02	16.87	16.63	18.52	15.65	14.87	11.99	13.17	15.20	26.79	26.57	9.06	14.83
MnO	0.07	0.07	0.15	0.17	0.18	0.17	0.17	0.14	0.13	0.14	0.25	0.23	0.13	0.11
NiO	0.02	<0.01	<0.01	<0.01	<0.01	<0.01	<0.01	<0.01	0.01	<0.01	<0.01	0.03	<0.01	0.01
MgO	7.96	9.60	13.89	14.18	12.73	14.87	13.89	13.73	13.36	13.05	15.88	15.91	<0.01	0.11
CaO	1.48	2.55	8.16	8.90	10.34	11.99	10.98	12.30	12.12	11.07	1.03	0.94	24.23	23.76
Na_2O	6.40	5.71	2.66	2.34	1.56	0.57	1.64	1.72	1.85	1.84	0.08	0.18	0.02	<0.01
K_2O	0.03	0.03	0.04	0.09	0.17	0.10	0.19	0.66	0.64	0.60	0.03	<0.01	<0.01	<0.01
F	0.03	<0.01	0.05	0.04	0.09	0.08	0.08	0.11	0.17	0.09	<0.01	<0.01	<0.01	<0.01
Total	99.21	98.09	99.36	99.02	99.04	99.04	98.92	99.08	99.24	99.23	90.38	90.30	98.96	98.61
Oxygen	13	13	13	13	13	13	13	13	13	13	28	28	12.5	12.5
Si	7.93	8.00	7.92	7.90	7.67	7.82	7.32	6.42	6.40	6.73	6.12	6.16	2.97	2.99
Ti	0.00	0.00	0.00	0.00	0.00	0.00	0.07	0.10	0.16	0.13	0.01	0.01	0.00	0.00
Al	0.67	0.50	0.31	0.26	0.50	0.25	0.99	2.27	2.17	1.83	4.19	4.16	2.53	2.07
Fe^{3+}	1.21	1.21	0.62	0.54	0.44	0.21	0.35	0.08	0.08	0.00	0.00	0.00	0.47	0.90
Fe^{2+}	1.46	1.39	1.19	1.25	1.59	1.49	1.26	1.23	1.37	1.69	4.22	4.18	0.00	0.00
Mn	0.01	0.01	0.02	0.02	0.02	0.02	0.02	0.02	0.02	0.02	0.04	0.04	0.01	0.01
Ni	0.00	0.00	0.00	0.00	0.00	0.00	0.00	0.00	0.00	0.00	0.00	0.01	0.00	0.00
Mg	1.72	1.89	2.95	3.03	2.77	3.20	2.99	2.97	2.91	2.87	4.95	4.95	0.00	0.00
Ca	0.23	0.27	1.24	1.37	1.62	1.86	1.70	1.91	1.90	1.75	0.23	0.21	2.02	2.02
Na	1.80	1.75	0.73	0.65	0.44	0.16	0.46	0.48	0.52	0.53	0.03	0.07	0.00	0.00
K	0.01	0.01	0.01	0.02	0.03	0.02	0.03	0.12	0.12	0.11	0.01	0.02	0.00	0.00
F	0.01	0.00	0.02	0.02	0.04	0.04	1.96	0.05	0.08	0.04	0.00	0.00	0.00	0.00
Total	15.03	15.02	14.98	15.03	15.09	15.03	15.19	15.61	15.64	15.64	19.80	19.80	8.00	7.99
X_{Mg}	0.54	0.58	0.71	0.71	0.64	0.68	0.70	0.71	0.68	0.63	0.54	0.54		
[IV]*Al*	0.07	0.60	0.08	0.10	0.33	0.18	0.68	1.58	1.60	1.27				
[VI]*Al*	0.00	0.50	0.23	0.16	0.17	0.07	0.31	0.69	0.57	0.55				

TABLE S3 Representative mineral analyses from hornblendite (sample OL02, site 1). Fe_2O_3* is the total amount of iron.

	Muscovite		Chlorite		Plagioclase		Epidote		Muscovite			Epidote		Plagioclase	
	OL25 mu	OL25 mu	OL25 chl	OL25 chl	OL25 ab	OL25 ab	OL25 ep core	OL25 ep rim	OL24 mu	OL24 mu	OL24 mu	OL24 ep rim	OL24 ep core	OL24 ab	OL24 ab
SiO_2	50.74	50.58	26.54	27.89	69.22	69.10	37.57	36.87	49.76	49.96	49.84	37.35	38.25	69.34	69.44
TiO_2	0.06	0.05	0.08	0.05	0.00	0.00	0.09	0.13	0.07	0.10	0.08	0.08	0.16	0.00	0.00
$Al2O_3$	24.79	23.60	19.88	20.06	19.57	19.83	24.80	21.78	27.35	25.22	26.93	22.93	26.25	19.66	19.58
Fe_2O_3*	5.02	6.13	25.27	23.96	0.04	<0.01	10.84	14.13	4.42	5.88	4.42	13.00	8.97	0.08	0.06
MnO	0.12	0.17	0.51	0.45	0.01	<0.01	0.16	0.55	0.15	0.15	0.16	0.39	0.13	<0.01	<0.01
NiO	<0.01	<0.01	<0.01	<0.01	<0.01	<0.01	<0.01	<0.01	<0.01	<0.01	<0.01	<0.01	<0.01	<0.01	<0.01
MgO	3.34	3.35	16.21	15.24	0.01	0.00	0.02	0.00	2.76	3.04	2.78	0.01	0.02	<0.01	<0.01
CaO	0.02	0.00	0.05	0.06	0.06	0.19	23.69	22.72	0.02	0.01	0.02	23.24	23.93	0.08	0.03
Na_2O	0.07	0.06	0.01	0.01	11.81	11.74	0.01	0.01	0.20	0.11	0.19	0.01	<0.01	11.75	11.88
K_2O	11.01	11.04	0.06	0.66	0.09	0.09	<0.01	<0.01	11.12	11.61	11.21	<0.01	<0.01	0.09	0.09
F	<0.01	<0.01	<0.01	<0.01	<0.01	<0.01	<0.01	<0.01	<0.01	<0.01	<0.01	<0.01	<0.01	<0.01	<0.01
Total	95.17	94.98	88.62	88.37	100.81	100.95	97.18	96.19	95.85	96.08	95.63	97.02	97.71	101.00	101.08
Oxygen	11	11	28	28	8	8	12.5	12.5	11	11	11	12.5	12.5	8	8
Si	3.46	3.48	5.63	5.87	3.00	2.99	2.99	3.01	3.36	3.41	3.38	3.00	3.00	3.00	3.00
Ti	0.00	0.00	0.01	0.01	0.00	0.00	0.01	0.01	0.00	0.01	0.00	0.01	0.01	1.00	0.00
Al	1.99	1.91	4.97	4.98	1.00	1.01	2.32	2.09	2.18	2.03	2.15	2.17	2.43	0.00	1.00
Fe^{3+}	0.00	0.00	0.00	0.00	0.00	0.00	0.65	0.87	0.00	0.00	0.00	0.79	0.53	0.00	0.00
Fe^{2+}	0.26	0.32	4.03	3.80	0.00	0.00	0.00	0.00	0.22	0.30	0.23	0.00	0.00	0.00	0.00
Mn	0.01	0.01	0.09	0.08	0.00	0.00	0.01	0.04	0.01	0.01	0.01	0.03	0.01	0.00	0.00
Ni	0.00	0.00	0.00	0.00	0.00	0.00	0.00	0.00	0.00	0.00	0.00	0.00	0.00	0.00	0.00
Mg	0.34	0.34	5.12	4.79	0.00	0.00	0.00	0.00	0.28	0.31	0.28	0.00	0.00	0.00	0.00
Ca	0.00	0.00	0.01	0.01	0.00	0.01	2.02	1.99	0.00	0.00	0.00	2.00	2.01	0.00	0.00
Na	0.01	0.01	0.01	0.00	0.99	0.99	0.01	0.02	0.03	0.02	0.02	0.00	0.01	0.99	1.00
K	0.96	0.97	0.02	0.18	0.01	0.01	0.00	0.00	0.96	1.01	0.97	0.00	0.00	0.01	0.01
F	0.00	0.00	0.00	0.00	0.00	0.00	0.00	0.00	0.00	0.00	0.00	0.00	0.00	0.00	0.00
Total	7.03	7.05	19.89	19.72	5.00	5.00	8.01	8.03	7.04	7.09	7.04	8.00	8.00	5.00	5.00
X_{Mg}	0.57	0.52	0.56	0.56					0.55	0.51	0.55				

TABLE S4 Representative mineral analyses from foliated and mylonitic orthogneisses (samples OL25 and OL24 respectively, site 2). Fe_2O_3* is the total amount of iron.

	Muscovite			Epidote		Plagioclase		Na amphibole				Na-Ca amphibole		Ca-amphibole		Epidote	
	OL23	OL23	OL23	OL23	OL23	OL23	OL23	OL50	OL50	OL50	OL50	OL50	OL50	OL50	OL50	OL50	OL50
	mu	mu	mu	ep core	ep rim	ab	ab	gl	gl	mrbk	mrbk	wnc	wnc	act	act	ep	ep
SiO_2	49.87	49.95	49.71	37.92	37.23	69.44	69.31	56.55	56.54	55.84	55.38	55.20	54.43	54.89	54.61	37.99	37.48
TiO_2	0.10	0.06	0.05	0.07	0.01	<0.01	<0.01	0.02	0.01	0.44	0.07	0.02	0.03	0.01	0.02	0.25	0.12
$Al2O_3$	25.31	25.47	26.44	25.62	22.25	19.58	19.74	5.89	6.42	4.56	4.00	1.80	1.96	1.38	1.67	26.52	23.41
Fe_2O_3*	6.11	5.90	5.31	9.92	14.09	0.06	0.01	19.55	19.04	20.04	22.05	16.64	16.08	14.97	15.34	8.27	13.25
MnO	0.14	0.18	0.15	0.21	0.28	<0.01	<0.01	0.22	0.24	0.27	0.23	0.44	0.52	0.56	0.53	0.23	0.48
NiO	<0.01	<0.01	<0.01	<0.01	<0.01	<0.01	<0.01	<0.01	<0.01	<0.01	<0.01	0.02	0.01	<0.01	<0.01	<0.01	<0.01
MgO	2.86	2.93	2.74	0.02	0.01	<0.01	<0.01	9.12	9.00	9.57	9.33	13.92	14.28	14.85	14.75	0.04	0.15
CaO	0.07	0.03	<0.01	23.94	23.08	0.03	0.13	0.66	0.55	1.33	1.43	8.24	9.41	11.20	10.52	23.89	22.95
Na_2O	0.12	0.10	0.14	0.01	0.01	11.88	11.79	6.87	7.03	6.55	6.53	2.70	1.99	0.91	1.37	0.02	<0.01
K_2O	11.22	11.32	11.63	<0.01	<0.01	0.09	0.07	<0.01	0.03	0.04	0.05	0.08	0.08	0.10	0.09	<0.01	<0.01
F	<0.01	<0.01	<0.01	<0.01	<0.01	<0.01	<0.01	0.07	0.07	0.06	0.09	0.10	0.12	0.12	0.12	<0.01	<0.01
Total	95.80	95.94	96.17	97.71	96.96	101.08	101.05	98.95	98.93	98.70	99.16	99.16	98.91	98.99	99.02	97.21	97.84
Oxygen	11	11	11	12.5	12.5	8	8	13	13	13	13	13	13	13	13	12.5	12.5
Si	3.41	3.41	3.38	2.99	3.01	3.00	3.00	7.99	7.98	7.97	7.93	7.89	7.81	7.89	7.84	2.99	2.98
Ti	0.00	0.00	0.00	0.00	0.00	0.00	0.00	0.00	0.00	0.05	0.01	0.00	0.00	0.00	0.00	0.02	0.01
Al	2.04	2.05	2.12	2.38	2.12	1.00	1.01	0.98	1.07	0.77	0.67	0.30	0.33	0.23	0.28	2.46	2.19
Fe^{3+}	0.00	0.00	0.00	0.59	0.86	0.00	0.00	0.95	0.86	0.98	1.20	0.63	0.58	0.25	0.40	0.49	0.79
Fe^{2+}	0.31	0.30	0.27	0.00	0.00	0.00	0.00	1.13	1.16	1.17	1.17	1.16	1.16	1.37	1.25	0.00	0.00
Mn	0.01	0.01	0.01	0.01	0.02	0.00	0.00	0.03	0.03	0.03	0.03	0.05	0.06	0.07	0.06	0.02	0.03
Ni	0.00	0.00	0.00	0.00	0.00	0.00	0.00	0.00	0.00	0.00	0.00	0.00	0.00	0.00	0.00	0.00	0.00
Mg	0.29	0.30	0.28	0.00	0.00	0.00	0.00	1.92	1.89	2.04	1.99	2.96	3.05	3.18	3.16	0.00	0.02
Ca	0.01	0.00	0.00	2.02	2.00	0.00	0.01	0.10	0.08	0.20	0.22	1.26	1.45	1.73	1.62	2.02	1.96
Na	0.02	0.01	0.02	0.02	0.01	1.00	0.99	1.88	1.92	1.81	1.81	0.75	0.55	0.25	0.38	0.01	0.00
K	0.98	0.98	1.01	0.00	0.00	0.01	0.00	0.00	0.00	0.01	0.01	0.02	0.01	0.02	0.02	0.00	0.00
F	0.00	0.00	0.00	0.00	0.00	0.00	0.00	0.03	0.03	0.03	0.04	0.05	0.06	0.06	0.05	0.00	0.00
Total	7.06	7.07	7.08	8.01	8.02	5.00	5.00	14.98	15.01	15.02	15.04	15.02	15.02	15.00	15.02	8.01	7.98
X_{Mg}	0.48	0.50	0.51					0.63	0.62	0.63	0.63	0.72	0.73	0.70	0.72		
[IV]*Al*								0.01	0.02	0.03	0.07	0.11	0.19	0.11	0.16		
[VI]*Al*								0.97	1.05	0.73	0.60	0.19	0.14	0.13	0.12		

TABLE S5 Representative mineral analyses from mylonitic orthogneisses and amphibole gneiss (samples OL23 and OL50, site 2). Fe_2O_3* is the total amount of iron.

	Na amphibole				Na-Ca amphibole		Ca amphibole		Na clinopyroxene		Epidote		Na amphibole	Na-Ca amphibole		Ca-amphibole		Epidote	
	OL68B	OL68B	OL68B	OL68B	OL68B	OL68B	OL68B	OL68B	OL68B	OL68B	OL68B	OL68B	OL61	OL61	OL61	OL61	OL61	OL61	OL61
	gl	gl	mrbk	mrbk	wnc	wnc	act	act	aeg-aug	aeg-aug	ep	ep	mrbk	wnc	wnc	act	act	ep	ep
SiO_2	56.58	55.62	55.05	54.27	55.88	54.72	53.01	53.56	54.41	54.28	38.14	37.77	56.13	55.84	55.53	53.03	55.26	37.43	37.53
TiO_2	0.37	0.02	0.11	0.09	0.06	<0.01	<0.01	<0.01	0.11	0.19	0.09	0.09	0.03	0.02	0.03	<0.01	0.01	0.10	0.10
$Al2O_3$	6.70	7.26	3.08	3.92	1.74	3.57	1.51	1.47	5.64	4.66	24.80	25.08	3.66	2.16	2.43	1.88	1.05	24.52	24.65
Fe_2O_3*	16.91	17.81	19.49	23.43	13.65	21.47	20.83	18.20	16.83	16.63	12.42	11.27	17.96	13.06	16.17	19.69	16.10	12.36	12.46
MnO	0.23	0.31	0.30	0.28	0.39	0.23	0.44	0.49	0.32	0.39	0.29	0.20	0.28	0.38	0.39	0.45	0.46	0.28	0.30
NiO	<0.01	<0.01	<0.01	<0.01	<0.01	<0.01	<0.01	<0.01	<0.01	<0.01	<0.01	<0.01	<0.01	0.02	<0.01	0.01	0.02	<0.01	<0.01
MgO	9.77	8.54	11.43	8.82	15.84	9.70	11.73	13.78	5.23	5.90	0.01	0.02	11.38	15.53	13.58	12.05	14.49	0.06	0.01
CaO	0.83	0.34	4.80	1.97	8.54	4.41	10.93	11.59	9.91	10.83	23.15	23.14	2.61	9.45	6.33	10.73	10.20	22.61	23.38
Na_2O	6.85	6.96	4.53	6.04	2.49	4.49	1.08	0.79	8.34	8.23	<0.01	<0.01	5.70	2.28	3.72	1.15	1.56	<0.01	<0.01
K_2O	<0.01	0.02	0.09	0.08	0.06	0.08	0.09	0.10	<0.01	<0.01	<0.01	<0.01	0.03	0.08	0.08	0.13	0.08	<0.01	<0.01
F	<0.01	0.07	<0.01	<0.01	<0.01	<0.01	<0.01	<0.01	<0.01	<0.01	<0.01	<0.01	<0.01	0.11	0.09	<0.01	0.06	<0.01	<0.01
Total	98.24	96.96	98.88	98.90	98.65	98.67	99.62	99.98	100.79	101.11	98.91	97.57	97.78	98.93	98.35	99.12	99.29	97.36	98.43
Oxygen	13	13	13	13	13	13	13	13	6	6	12.5	12.5	13	13	13	13	13	12.5	12.5
Si	7.97	7.98	7.89	7.84	7.88	7.93	7.95	7.85	2.00	1.99	2.99	2.99	8.00	7.92	7.92	7.80	7.93	2.97	2.96
Ti	0.04	0.00	0.01	0.01	0.01	0.00	0.00	0.00	0.00	0.01	0.01	0.01	0.00	0.00	0.00	0.00	0.00	0.01	0.01
Al	1.11	1.23	0.52	0.67	0.29	0.61	0.27	0.25	0.25	0.20	2.29	2.34	0.62	0.36	0.41	0.33	0.18	2.29	2.29
Fe^{3+}	0.74	0.76	0.93	1.31	0.67	0.89	0.00	0.00	0.34	0.39	0.73	0.67	0.99	0.29	0.77	0.35	0.38	0.74	0.74
Fe^{2+}	1.06	1.16	1.17	1.24	0.78	1.45	2.35	2.01	0.13	0.07	0.00	0.00	0.93	1.10	0.97	1.83	1.36	0.00	0.00
Mn	0.03	0.04	0.04	0.03	0.05	0.03	0.06	0.06	0.01	0.01	0.02	0.00	0.03	0.05	0.05	0.06	0.06	0.02	0.02
Ni	0.00	0.00	0.00	0.00	0.00	0.00	0.00	0.00	0.00	0.00	0.00	0.00	0.00	0.00	0.00	0.00	0.00	0.00	0.00
Mg	2.05	1.83	2.44	1.90	3.33	2.09	2.62	3.01	0.29	0.32	0.00	0.00	2.42	3.28	2.89	2.64	3.10	0.01	0.00
Ca	0.13	0.05	0.74	0.30	1.29	0.68	1.76	1.82	0.39	0.43	1.95	1.96	0.40	1.44	0.97	1.69	1.57	1.92	1.98
Na	1.87	1.94	1.26	1.69	0.68	1.26	0.31	0.22	0.60	0.59	0.00	0.00	1.58	0.63	1.03	0.33	0.43	0.00	0.00
K	0.00	0.00	0.02	0.01	0.01	0.01	0.02	0.02	0.00	0.00	0.00	0.00	0.01	0.01	0.01	0.01	0.01	0.00	0.00
F	0.00	0.03	0.00	0.00	0.00	0.00	0.00	0.00	0.00	0.00	0.00	0.00	0.00	0.05	0.04	0.00	0.03	0.00	0.00
Total	15.00	14.99	15.02	15.00	14.98	14.96	15.34	15.24	4.00	4.00	7.99	7.97	14.98	15.08	15.01	15.04	15.02	7.96	8.00
X_{Mg}	0.74		0.68	0.63	0.81	0.59	0.53	0.15	0.69	0.82			0.72	0.75	0.62	0.59	0.70		
[IV]*Al*	0.03		0.11	0.07	0.12	0.07	0.05	0.10	0.00	0.01			0.00	0.08	0.08	0.20	0.07		
[VI]*Al*	0.50		0.41	0.91	0.17	0.54	0.22	0.60	0.25	0.19			0.62	0.28	0.33	0.12	0.1		
Quad									0.18	0.19									
Aeg									0.34	0.39									
Jd									0.48	0.40									

TABLE S6 Representative mineral analyses from amphibole gneisses (samples OL68A, OL68B and OL61, sites 2 and 3). Fe_2O_3* is the total amount of iron.

	Chlorite					Muscovite			Epidote		Na-Ca amphibole		Chlorite				Plagioclase	
	OL49C		OL49A			OL49B			OL49C		OL42A		OL42A		OL42B		OL42A	
	chl	chl	chl	chl core	chl rim	mu	mu	mu	ep	ep	wnc	wnc	chl	chl	chl	chl	ab	ab
SiO_2	26.57	26.82	29.54	27.33	28.61	48.83	50.58	49.57	37.31	37.47	55.02	55.11	27.00	27.15	29.49	28.74	68.95	68.83
TiO_2	0.02	0.02	0.02	0.01	<0.01	0.07	0.04	0.06	0.07	0.25	0.07	<0.01	<0.01	<0.01	<0.01	<0.01	<0.01	<0.01
$Al2O_3$	20.76	20.41	20.57	19.64	19.93	28.40	27.38	27.14	22.85	22.63	2.01	2.09	18.90	18.91	19.14	19.45	19.52	19.53
Fe_2O_3*	19.39	18.70	8.45	16.42	11.60	3.04	2.74	2.76	13.35	13.39	11.63	13.64	22.30	20.70	11.27	13.62	0.01	0.03
MnO	0.37	0.40	0.19	0.31	0.27	0.03	0.01	0.02	0.17	0.15	0.19	0.23	0.26	0.28	0.20	0.23	<0.01	<0.01
NiO	<0.01	<0.01	<0.01	<0.01	<0.01	<0.01	<0.01	<0.01	<0.01	<0.01	<0.01	<0.01	<0.01	<0.01	<0.01	<0.01	<0.01	<0.01
MgO	20.89	21.12	28.50	22.81	26.43	3.32	2.87	3.66	0.01	0.03	16.52	15.52	19.82	20.74	27.55	25.72	<0.01	<0.01
CaO	0.04	0.03	0.02	0.04	0.04	0.04	0.01	0.01	23.34	23.31	9.63	10.10	0.01	0.03	0.02	0.01	0.02	0.02
Na_2O	0.03	<0.01	0.01	0.01	0.01	0.20	1.43	0.16	<0.01	0.01	2.02	1.88	0.01	0.03	<0.01	<0.01	11.75	11.79
K_2O	0.02	0.01	<0.01	0.01	<0.01	11.46	10.57	11.59	<0.01	<0.01	0.14	0.15	0.01	<0.01	<0.01	<0.01	0.05	0.04
F	<0.01	<0.01	<0.01	<0.01	<0.01	<0.01	<0.01	<0.01	<0.01	<0.01	0.05	0.06	<0.01	<0.01	<0.01	<0.01	<0.01	<0.01
Total	88.09	87.51	87.30	86.58	86.89	95.39	95.63	94.97	97.09	97.23	97.28	98.78	88.31	87.84	87.67	87.77	100.30	100.24
Oxygen	28	28	28	28	28	11	11	11	12.5	12.5	13	13	28	28	28	28	8	8
Si	5.47	5.54	5.72	5.63	5.69	3.30	3.39	3.36	3.00	3.01	7.86	7.86	5.64	5.65	5.79	5.72	3.00	3.00
Ti	0.00	0.00	0.00	0.00	0.00	0.00	0.00	0.00	0.00	0.01	0.01	0.00	0.00	0.00	0.00	0.00	0.00	0.00
Al	5.04	4.96	4.70	4.76	4.67	2.26	2.16	2.17	2.17	2.14	0.34	0.35	4.66	4.64	4.43	4.56	1.00	1.00
Fe^{3+}	0.00	0.00	0.00	0.00	0.00	0.00	0.00	0.00	0.81	0.81	0.39	0.30	0.00	0.00	0.00	0.00	0.00	0.00
Fe^{2+}	3.00	2.90	1.23	2.54	1.73	0.15	0.14	0.14	0.00	0.00	0.86	1.17	3.50	3.24	1.66	2.04	0.00	0.00
Mn	0.07	0.07	0.03	0.05	0.05	0.00	0.00	0.00	0.01	0.00	0.02	0.03	0.05	0.05	0.03	0.04	0.00	0.00
Ni	0.00	0.00	0.00	0.00	0.00	0.00	0.00	0.00	0.00	0.00	0.00	0.00	0.00	0.00	0.00	0.00	0.00	0.00
Mg	6.41	6.50	8.23	7.00	7.83	0.33	0.29	0.37	0.00	0.00	3.52	3.30	6.18	6.44	8.07	7.63	0.00	0.00
Ca	0.01	0.01	0.00	0.01	0.01	0.00	0.00	0.00	2.01	2.01	1.47	1.54	0.00	0.01	0.00	0.00	0.00	0.00
Na	0.01	0.00	0.00	0.00	0.00	0.03	0.19	0.02	0.01	0.03	0.56	0.52	0.00	0.01	0.00	0.00	0.99	1.00
K	0.01	0.00	0.00	0.00	0.00	0.99	0.90	1.00	0.00	0.00	0.03	0.03	0.00	0.00	0.00	0.00	0.00	0.00
F	0.00	0.00	0.00	0.00	0.00	0.00	0.00	0.00	0.00	0.00	0.02	0.03	0.00	0.00	0.00	0.00	0.00	0.00
Total	20.02	19.98	19.93	20.00	19.98	7.08	7.07	7.06	8.01	8.01	15.06	15.09	20.03	20.03	19.99	20.00	5.00	5.00
X_{Mg}	0.68	0.69	0.87	0.73	0.82	0.68	0.68	0.72			0.80	0.74	0.64	0.67	0.83	0.79		
[IV]*Al*											0.14	0.14						
[VI]*Al*											0.20	0.21						

TABLE S7 Representative mineral analyses from amphibole gneiss (sample OL49C, site 2), metatonalite (sample OL42A, site 6) and chlorite-schist (samples OL49A, OL42B, sites 2 and 6 respectively). Fe_2O_3* is the total amount of iron.

	Na amphibole		Na-Ca amphibole		Albite		Na amphibole		Na-Ca amphibole		Ca amphibole		Na clinopyroxene		Magmatic muscovite		Plagioclase	
	OL40		OL40		OL40		OL43		OL43		OL43		OL43		OL43		OL43	
	mrbk	mrbk	wnc	wnc	ab	ab	mrbk	mrbk	wnc	wnc	act	act	aeg-aug	aeg-aug	mu	mu	ab	ab
SiO_2	55.27	54.99	56.02	55.77	68.68	68.82	54.92	56.30	54.60	55.45	55.78	56.06	54.36	54.56	46.35	46.54	68.68	68.84
TiO_2	0.06	0.04	0.00	0.02	0.00	0.00	0.05	0.03	0.04	0.02	0.05	0.07	0.06	0.08	0.61	0.69	0.00	0.00
$Al2O_3$	4.27	3.66	0.57	1.00	19.69	19.79	3.32	3.09	2.48	2.48	1.33	1.30	5.18	5.67	31.73	31.02	19.69	19.59
Fe_2O_3*	21.79	23.64	14.88	16.23	<0.01	0.04	22.66	19.65	22.47	20.25	12.28	12.58	15.73	15.57	4.67	5.06	<0.01	<0.01
MnO	0.23	0.22	0.33	0.40	<0.01	<0.01	0.30	0.23	0.34	0.43	0.39	0.43	0.22	0.24	0.04	0.04	<0.01	<0.01
NiO	<0.01	<0.01	<0.01	<0.01	<0.01	<0.01	0.01	<0.01	<0.01	0.02	<0.01	0.01	<0.01	<0.01	<0.01	<0.01	<0.01	<0.01
MgO	8.89	8.52	15.44	14.58	<0.01	<0.01	9.11	11.06	10.07	11.31	16.39	16.32	6.11	5.80	1.16	1.28	<0.01	<0.01
CaO	1.36	1.49	9.39	7.60	0.19	0.21	3.03	2.59	4.78	4.93	11.82	12.24	10.82	10.40	<0.01	<0.01	0.19	<0.01
Na_2O	6.44	6.37	1.95	3.05	11.42	11.61	5.43	5.89	4.41	4.41	0.68	0.50	8.07	8.37	0.21	0.24	11.42	11.72
K_2O	0.03	0.04	0.04	0.06	0.09	0.07	0.06	0.05	0.07	0.07	0.05	0.04	0.03	<0.01	11.33	11.47	0.09	0.05
F	<0.01	<0.01	0.01	0.02	<0.01	<0.01	0.01	<0.01	0.01	<0.01	<0.01	<0.01	<0.01	<0.01	<0.01	<0.01	<0.01	<0.01
Total	98.34	98.97	98.63	98.73	100.07	100.54	98.90	98.89	99.27	99.37	98.77	99.55	100.58	100.69	96.10	96.34	100.07	100.20
Oxygen	13	13	13	13	8	8	13	13	13	13	13	13	6	6	11	11	8	8
Si	7.96	7.94	7.99	7.95	2.99	2.99	7.95	8.00	7.91	7.93	7.94	7.94	2.00	2.00	3.14	3.16	2.99	3.00
Ti	0.01	0.00	0.00	0.00	0.00	0.00	0.01	0.00	0.00	0.00	0.01	0.01	0.00	0.00	0.03	0.04	0.00	0.00
Al	0.73	0.62	0.10	0.17	1.01	1.01	0.57	0.52	0.42	0.42	0.22	0.22	0.22	0.24	2.53	2.48	1.01	1.01
Fe^{3+}	1.11	1.23	0.51	0.76	0.00	0.00	1.04	1.04	1.02	0.96	0.10	0.03	0.36	0.35	0.00	0.00	0.00	0.00
Fe^{2+}	1.25	1.34	1.08	0.98	0.00	0.00	1.43	1.06	1.43	1.22	1.22	1.31	0.08	0.08	0.24	0.26	0.00	0.00
Mn	0.03	0.03	0.04	0.05	0.00	0.00	0.04	0.03	0.04	0.05	0.05	0.05	0.01	0.01	0.00	0.00	0.00	0.00
Ni	0.00	0.00	0.00	0.00	0.00	0.00	0.00	0.00	0.00	0.00	0.00	0.00	0.00	0.00	0.00	0.00	0.00	0.00
Mg	1.91	1.83	3.28	3.10	0.00	0.00	1.97	2.34	2.17	2.41	3.48	3.44	0.33	0.32	0.12	0.13	0.00	0.00
Ca	0.21	0.23	1.43	1.16	0.01	0.01	0.47	0.39	0.74	0.76	1.80	1.86	0.43	0.41	0.00	0.00	0.01	0.00
Na	1.80	1.78	0.51	0.85	0.97	0.98	1.52	1.62	1.24	1.22	0.19	0.14	0.57	0.59	0.03	0.03	0.97	0.99
K	0.01	0.01	0.01	0.01	0.01	0.00	0.01	0.01	0.01	0.01	0.01	0.01	0.00	0.00	0.98	0.99	0.01	0.00
F	0.00	0.00	0.00	0.01	0.00	0.00	0.00	0.00	0.01	0.00	0.00	0.00	0.00	0.00	0.00	0.00	0.00	0.00
Total	15.01	15.02	14.98	15.01	4.99	5.00	15.01	15.03	14.99	14.99	15.00	15.00	4.00	4.00	7.07	7.08	4.99	5.00
X_{Mg}	0.6	0.58	0.75	0.05			0.58	0.69	0.60	0.66	0.74	0.73	0.81	0.80	0.33	0.33		
[IV]*Al*	0.04	0.06	0.01	0.11			0.05	0.00	0.09	0.07	0.06	0.06	0.00	0.00				
[VI]*Al*	0.69	0.57	0.08	0.76			0.52	0.52	0.33	0.35	0.16	0.15	0.22	0.24				
												Quad	0.42	0.40				
												Aeg	0.36	0.35				
												Jd	0.22	0.24				

TABLE S8 Representative mineral analyses from metatonalite (samples OL40 and OL43, site 6). Fe_2O_3* is the total amount of iron.

	Na amphibole		Na-Ca amphibole		Na clinopyroxene		Epidote		Plagioclase		Epidote			Chlorite		Muscovite		Albite	
	OL44		OL44		OL44		OL44		OL44		OL1424			OL1424		OL1424		OL1424	
	mrbk	mrbk	wnc	wnc	aeg-aug	aeg-aug	ep core	ep rim	ab	ab	zo	zo	zo	chl	chl	mu	mu	ab	ab
SiO_2	55.17	55.04	55.48	55.98	54.02	54.31	38.05	37.80	68.73	68.77	39.54	39.59	39.56	28.85	28.27	51.53	49.93	67.91	68.39
TiO_2	0.06	0.05	0.07	0.10	0.10	0.10	0.03	0.10	<0.01	<0.01	0.09	0.03	<0.01	<0.01	0.03	0.02	0.04	0.01	<0.01
$Al2O_3$	3.73	4.68	3.87	3.30	4.41	5.29	27.13	24.50	19.71	19.66	34.15	34.10	33.66	21.85	22.55	27.59	32.41	19.30	19.75
Fe_2O_3*	21.46	22.47	22.07	20.02	15.97	14.87	8.06	11.16	0.07	<0.01	0.23	0.48	0.82	11.85	8.81	1.10	0.64	<0.01	0.01
MnO	0.23	0.21	0.24	0.26	0.21	0.26	0.01	0.25	<0.01	<0.01	<0.01	<0.01	0.01	0.08	0.07	<0.01	0.01	0.01	0.02
NiO	<0.01	0.03	<0.01	0.03	<0.01	<0.01	<0.01	<0.01	<0.01	<0.01	<0.01	<0.01	<0.01	<0.01	<0.01	<0.01	<0.01	<0.01	<0.01
MgO	9.39	8.57	9.42	10.81	6.50	6.72	0.02	0.03	<0.01	<0.01	<0.01	<0.01	0.01	26.30	27.29	3.87	2.67	<0.01	<0.01
CaO	3.03	1.83	2.91	3.28	12.42	12.13	23.83	23.70	0.19	0.16	24.94	24.90	24.85	0.02	0.04	0.01	0.01	0.13	0.32
Na_2O	5.57	6.13	5.36	5.22	7.12	7.23	0.01	0.01	11.70	11.61	0.02	0.01	0.02	0.01	<0.01	0.23	0.31	11.46	11.42
K_2O	0.07	0.04	0.06	0.07	0.02	0.01	<0.01	<0.01	0.06	0.06	<0.01	<0.01	<0.01	0.04	<0.01	10.84	10.55	0.04	0.03
F	<0.01	<0.01	<0.01	<0.01	<0.01	<0.01	<0.01	<0.01	<0.01	<0.01	<0.01	<0.01	<0.01	<0.01	<0.01	<0.01	<0.01	<0.01	<0.01
Total	98.71	99.05	99.48	99.07	100.77	100.92	97.15	97.55	100.46	100.26	98.97	99.10	98.93	88.99	87.05	95.19	96.57	98.87	99.94
Oxygen	13	13	13	13	6	6	12.5	12.5	8	8	12.5	12.5	12.5	28	28	11	11	8	8
Si	7.97	7.91	7.93	7.97	1.99	1.99	2.99	3.00	2.99	2.99	2.96	2.97	2.97	5.59	5.50	3.42	3.26	3.00	2.99
Ti	0.01	0.01	0.01	0.01	0.00	0.00	0.00	0.01	0.00	0.00	0.00	0.00	0.00	0.00	0.00	0.00	0.00	0.00	0.00
Al	0.64	0.79	0.65	0.55	0.19	0.23	2.52	2.29	1.01	1.01	3.00	2.99	2.98	4.99	5.17	2.16	2.49	1.00	1.02
Fe^{3+}	0.89	1.10	1.09	1.04	0.32	0.30	0.48	0.67	0.00	0.00	0.03	0.05	0.05	0.00	0.00	0.00	0.00	0.00	0.00
Fe^{2+}	1.44	1.33	1.29	1.10	0.12	0.11	0.00	0.00	0.00	0.00	0.00	0.00	0.00	1.73	1.29	0.06	0.03	0.00	0.00
Mn	0.03	0.03	0.03	0.03	0.01	0.01	0.00	0.02	0.00	0.00	0.00	0.00	0.00	0.01	0.01	0.00	0.00	0.00	0.00
Ni	0.00	0.00	0.00	0.00	0.00	0.00	0.00	0.00	0.00	0.00	0.00	0.00	0.00	0.00	0.00	0.00	0.00	0.00	0.00
Mg	2.02	1.84	2.01	2.29	0.36	0.37	0.00	0.00	0.00	0.00	0.00	0.00	0.00	7.59	7.92	0.38	0.26	0.00	0.00
Ca	0.47	0.28	0.45	0.50	0.49	0.48	2.01	2.01	0.01	0.01	2.00	2.00	2.00	0.00	0.01	0.00	0.00	0.01	0.15
Na	1.56	1.71	1.49	1.44	0.51	0.51	0.02	0.02	0.99	0.98	0.00	0.00	0.03	0.00	0.00	0.03	0.04	0.98	0.97
K	0.01	0.01	0.01	0.01	0.00	0.00	0.00	0.00	0.00	0.00	0.00	0.00	0.00	0.01	0.00	0.92	0.88	0.00	0.00
F	0.00	0.00	0.00	0.00	0.00	0.00	0.00	0.00	0.00	0.00	0.00	0.00	0.00	0.00	0.00	0.00	0.00	0.00	0.00
Total	15.04	15.00	14.94	14.95	4.00	4.00	8.02	8.02	5.00	4.99	7.99	8.00	8.02	19.92	19.91	6.97	6.96	4.99	4.99
X_{Mg}	0.58	0.58	0.61	0.68	0.75	0.76								0.81	0.86	0.87	0.89		
[IV]*Al*	0.03	0.09	0.07	0.03	0.01	0.01								2.41	2.50				
[VI]*Al*	0.61	0.70	0.58	0.52	0.19	0.22								2.58	2.68				
Quad					0.48	0.48													
Aeg					0.32	0.29													
Jd					0.19	0.22													

TABLE S9 Representative mineral analyses from a metatonalite (sample OL44, site 6) and a leucocratic metagabbro (OL1424, site 4). Fe_2O_3* is the total amount of iron.

	Na amphibole				Muscovite		Chlorite		Epidote		Garnet	
	VP7				VP7		VP7		VP7		VP7	
	gl	gl	mrbk	mrbk	mu	mu	chl	chl	ep	ep	g	g
SiO_2	54.80	54.34	53.95	53.74	49.27	49.44	25.45	26.45	37.95	37.51	36.63	36.20
TiO_2	0.07	0.04	0.03	0.01	0.08	0.09	0.02	0.14	0.06	0.06	0.10	0.11
$Al2O_3$	5.73	6.00	5.73	4.58	25.51	26.11	19.35	19.21	26.56	23.66	20.78	20.32
Fe_2O_3*	21.96	22.34	23.15	22.30	5.56	5.02	28.24	26.94	8.99	12.43	11.54	11.30
MnO	0.33	0.35	0.37	0.46	0.06	0.05	0.96	0.83	0.13	0.06	22.77	22.89
NiO	<0.01	0.03	<0.01	0.02	<0.01	<0.01	<0.01	<0.01	<0.01	<0.01	<0.01	<0.01
MgO	7.25	7.00	6.79	8.41	2.86	2.93	14.24	13.74	0.01	0.01	0.19	0.17
CaO	0.50	0.69	0.92	1.68	0.01	<0.01	0.03	0.09	23.94	23.60	8.65	8.65
Na_2O	6.86	6.83	6.62	6.13	0.21	0.24	0.03	0.02	<0.01	0.01	<0.01	<0.01
K_2O	<0.01	0.04	0.06	0.07	11.24	11.22	0.02	0.71	<0.01	<0.01	<0.01	<0.01
F	0.04	0.06	0.04	0.05	<0.01	<0.01	<0.01	<0.01	<0.01	<0.01	<0.01	<0.01
Total	97.54	97.70	97.66	97.45	94.80	95.11	88.34	88.13	97.64	97.33	100.65	99.64
Oxygen	13	13	13	13	11	11	28	28	12.5	12.5	12	12
Si	7.98	7.94	7.92	7.86	3.39	3.38	5.55	5.74	2.97	2.97	2.97	2.97
Ti	0.01	0.00	0.00	0.00	0.00	0.00	0.00	0.02	0.00	0.00	0.01	0.01
Al	0.98	1.03	0.99	0.79	2.07	2.11	4.97	4.91	2.08	2.20	1.99	1.96
Fe^{3+}	0.93	0.93	0.98	1.21	0.00	0.00	0.00	0.00	0.96	0.82	0.07	0.09
Fe^{2+}	1.48	1.53	1.57	1.25	0.29	0.26	4.63	4.40	0.00	0.00	0.64	0.60
Mn	0.04	0.04	0.05	0.06	0.00	0.00	0.18	0.15	0.05	0.00	1.56	1.59
Ni	0.00	0.00	0.00	0.00	0.00	0.00	0.00	0.00	0.00	0.00	0.00	0.00
Mg	1.57	1.52	1.49	1.83	0.29	0.30	4.63	4.44	0.00	0.00	0.02	0.02
Ca	0.08	0.11	0.14	0.26	0.00	0.00	0.01	0.02	1.94	2.00	0.75	0.76
Na	1.94	1.93	1.88	1.74	0.03	0.03	0.01	0.01	0.00	0.00	0.00	0.00
K	0.00	0.01	0.01	0.01	0.99	0.98	0.01	0.20	0.00	0.00	0.00	0.00
F	0.00	0.03	0.02	0.02	0.00	0.00	0.00	0.00	0.00	0.00	0.00	0.00
Total	15.01	15.05	15.04	15.01	7.06	7.06	19.98	19.89	8.00	7.99	8.00	8.00
X_{Mg}	0.52	0.50	0.49	0.59	0.50	0.54	0.50	0.50		py	1	1
[IV]*Al*	0.02	0.06	0.08	0.14				2.26		alm	21	20
[VI]*Al*	0.97	0.97	0.91	0.65				2.65		grs	22	21
										spss	53	53
										andr	3	5

TABLE S10 Representative mineral analyses from blueschist (sample VP7, site 7). Fe_2O_3* is the total amount of iron.

	Site 1			Site 2											
Rock type	Hornblendite			Foliated orthogneiss	Mylonitic orthogneiss		Am-gneiss				Mu-rich layer	Chlorite-schist	Ultramafic cumulate		
Sample	OL02	OL03	OL04	OL25	OL24	OL23	OL50	OL68B	OL68A	OL49C	OL49B	OL49A	OL35	OL34	OL33
SiO_2	42.08	36.41	37.56	71.19	61.75	64.81	72.39	62.06	59.67	62.63	44.56	28.78	43.69	51.36	39.82
Al_2O_3	17.52	16.30	12.00	14.66	17.65	16.65	14.21	17.22	18.01	19.48	21.56	19.93	2.16	1.63	10.16
Fe_2O_3*	13.01	18.27	21.92	2.72	5.11	4.04	2.78	4.92	5.52	2.00	6.92	10.92	16.29	10.60	9.04
MnO	0.12	0.14	0.15	0.05	0.09	0.08	0.05	0.08	0.09	0.04	0.18	0.30	0.15	0.07	0.10
MgO	7.49	6.52	9.01	0.97	1.68	1.47	0.50	1.37	1.75	1.08	12.07	25.92	29.90	29.32	28.55
CaO	11.38	14.72	10.45	0.62	2.77	2.76	2.88	4.81	4.12	2.01	2.14	1.46	0.05	bdl	4.08
Na_2O	1.88	0.39	0.72	5.24	6.85	6.35	6.32	8.56	8.04	9.97	3.54	bdl	bdl	bdl	0.05
K_2O	0.73	bdl	bdl	2.54	1.18	1.12	0.39	0.03	0.33	0.41	2.18	bdl	bdl	bdl	bdl
TiO_2	0.99	1.99	2.34	0.33	0.63	0.48	0.28	0.63	0.71	0.45	0.72	1.05	0.05	bdl	0.03
P_2O_5	bdl	bdl	bdl	bdl	0.17	0.12	bdl	0.16	0.18	0.12	0.17	0.25	bdl	bdl	bdl
LOI	3.79	3.98	5.48	1.20	2.13	1.65	0.88	0.75	1.60	1.24	6.39	11.26	8.21	6.51	8.45
Total	98.98	98.72	99.63	99.52	100.01	99.53	100.68	100.58	100.02	99.42	100.42	99.86	100.51	99.48	100.27
FeO	6.50	7.52	9.95	0.81	1.82	1.57	0.67	0.61	0.45	0.73	4.47	8.94	6.93	5.02	5.46
Fe^3/Fe*	0.29	0.37	0.33	0.50	0.40	0.43	0.82	0.78	0.65	0.42	0.16	0.05	0.36	0.31	0.20
Mg#	67	61	62	68	62	63	64	70	63	72	83	84	88	91	90

TABLE S11: Bulk geochemical data of the studied samples from the DBTS. Major elements reported in oxide wt.%. Mg# and ratio Fe^3/Fe* are reported in molar percent. Fe_2O_3* is the total amount of iron. LOI = loss on ignition.

	Site 4	Site 5	Site 3		Site 5		Site 4	Site 5	Site 6							Site 7	Diehl et al. 1952
Rock type	Ultramafic cumulate	Orthogneiss	Am-gneiss					Leucocratic metagabbro	Metatonalite				Chlorite-schist	Ultramafic cumulate		Blueschist	Orthogneiss
Sample	OL60	OL08	OL61	OL62	OL63	OL06	OL21A	OL21B	OL1424	OL39	OL40	OL43	OL42A	OL42B	OL54	OL55	VP7	14
SiO_2	38.88	68.20	70.72	72.42	55.89	66.99	76.35	70.77	45.45	68.79	72.01	72.61	60.50	29.23	37.34	42.09	57.92	65.51
Al_2O_3	5.77	15.85	14.58	13.60	18.37	17.87	13.45	13.83	28.66	15.62	14.41	14.39	19.19	18.66	2.32	1.08	15.38	15.82
Fe_2O_3*	10.02	3.62	2.86	2.22	6.13	1.70	0.57	2.57	0.97	2.45	1.99	1.61	3.26	13.59	13.12	6.19	9.09	4.61
MnO	0.12	0.07	0.05	0.04	0.11	0.02	bdl	0.05	0.02	0.03	0.02	0.03	0.06	0.29	0.13	0.19	0.18	0.13
MgO	33.11	1.41	0.74	0.58	2.32	1.10	0.23	0.80	1.99	1.57	1.18	1.07	4.27	25.95	34.47	38.11	2.61	1.49
CaO	0.40	1.99	2.92	2.13	6.55	0.61	0.47	3.18	16.41	1.01	0.56	0.74	0.48	0.57	0.05	bdl	3.84	3.00
Na_2O	bdl	4.83	7.62	6.83	7.36	10.74	8.01	7.13	2.14	9.71	9.05	8.76	9.63	0.02	bdl	bdl	2.76	4.06
K_2O	bdl	2.35	0.03	0.39	0.04	0.05	0.04	0.04	0.69	0.07	0.04	0.09	bdl	bdl	bdl	bdl	3.65	2.83
TiO_2	0.06	0.47	0.31	0.25	0.79	0.24	0.07	0.36	0.06	0.29	0.29	0.18	0.41	0.48	0.08	0.02	1.39	1.23
P_2O_5	bdl	0.15	bdl	bdl	0.21	bdl	bdl	bdl	bdl	bdl	bdl	bdl	bdl	0.16	bdl	bdl	0.48	0.02
LOI	11.11	1.71	0.70	0.79	1.64	0.78	0.35	0.75	2.38	0.45	0.56	0.81	2.28	11.13	11.57	12.05	2.96	1.40
Total	99.46	100.64	100.52	99.24	99.40	100.09	99.53	99.47	98.76	99.97	100.11	100.28	100.08	100.08	99.06	99.73	100.27	99.88
FeO	4.60	1.86	0.51	0.41	1.36	0.62	0.12	0.45	0.61	1.21	0.77	0.84	2.54	11.6	5.09	4.16	2.79	2.49
Fe^3/Fe*	0.32	0.27	0.67	0.66	0.70	0.42	0.62	0.67	0.18	0.29	0.40	0.27	0.07	0.03	0.40	0.15	0.49	0.26
Mg#	93	57	72	71	75	76	77	76	85	70	73	69	75	80	92	94	63	52

TABLE S12: Bulk geochemical data of the studied samples from the DBTS. Major elements reported in oxide wt.%. Mg# and ratio Fe^3/Fe* are reported in molar percent. Fe_2O_3* is the total amount of iron. LOI = loss on ignition.

	Site 1			Site 2												
Rock type	Hornblendite			Foliated orthogneiss	Mylonitic orthogneiss		Am-gneiss				Mu-rich layer	Chlorite-schist	Ultramafic cumulate		
Sample	OL02	OL03	OL04	OL25	OL24	OL23	OL50	OL68B	OL68A	OL49C	OL49B	OL49A	OL35	OL34	OL33
Trace elements (ppm)															
As	bdl	1.51	1.91	bdl	bdl	bdl	bdl	bdl	bdl	bdl	bdl	bdl	bdl	bdl	bdl
Ba	217	22	11	401	165	227	47	3.80	44	49	283	bdl	bdl	bdl	bdl
Be	0.42	0.47	0.59	2.71	2.41	2.43	1.37	2.13	2.00	0.53	1.04	0.43	0.34	0.13	0.37
Bi	bdl	bdl	0.07	0.09	0.05	0.10	bdl	bdl	bdl	0.07	bdl	bdl	0.06	bdl	bdl
Cd	0.07	0.11	0.05	0.04	0.07	0.07	0.04	0.22	0.20	0.05	0.06	0.07	0.03	0.04	0.06
Co	38	66	92	5.91	5.70	4.91	1.12	4.68	4.27	3.10	12	19	153	83	100
Cr	103	45	15	5.43	3.78	3.79	3.73	bdl	bdl	5.54	6.14	6.36	5735	1943	2318
Cs	0.15	0.04	0.08	0.81	0.47	0.37	0.14	bdl	0.10	0.12	0.68	0.04	0.18	0.15	0.25
Cu	39	87	61	bdl	18	4.54	3.21	bdl	8.85	6.48	12	9.57	50	65	27
Ga	21	26	21	19	21	20	18	23	23	18	21	17	3.98	2.34	7.75
Ge	1.12	1.76	1.26	1.24	1.11	1.26	1.05	1.50	1.36	0.67	0.83	0.76	0.82	0.97	0.82
Hf	0.57	0.69	0.98	5.20	7.10	5.22	4.03	7.51	7.72	4.62	6.99	10	0.07	bdl	0.04
In	0.07	0.07	0.09	0.03	0.05	0.05	bdl	bdl	bdl	0.04	0.06	0.06	bdl	bdl	bdl
Mo	bdl	bdl	bdl	bdl	1.05	bdl	1.03	bdl	0.86	bdl	bdl	bdl	bdl	bdl	bdl
Nb	0.58	1.60	2.20	11	10	11	6.09	10	11	11	16	15	1.08	0.20	0.57
Ni	15	16	20	bdl	bdl	bdl	bdl	bdl	bdl	2.27	2.78	2.87	1585	1318	1232
Pb	2.10	3.92	3.13	4.12	18	12	14	15	19	13	13	3.32	0.83	1.07	0.91
Rb	19	0.60	0.64	83	41	39	13	bdl	11	16	94	0.74	0.20	0.30	0.38
Sc	76	63	94	6.99	14	11	4.12	13	14	12	16	21	5.58	3.72	5.44
Sb	0.80	1.91	2.58	1.16	0.26	0.23	0.19	bdl	0.23	0.23	0.26	0.08	0.41	0.09	0.07
Sn	bdl	bdl	bdl	2.46	2.14	2.85	1.94	1.95	2.64	3.84	4.74	3.01	0.66	bdl	0.40
Sr	377	557	327	71	367	273	377	638	718	412	444	141	0.97	1.16	6.12
Ta	0.08	0.19	0.19	0.99	1.10	0.98	0.79	0.81	1.19	0.97	2.07	1.30	0.04	0.01	0.02
Th	0.07	0.26	0.21	16	9.71	11	13	8.36	7.47	12	16	6.33	0.32	0.23	0.10
U	0.04	0.15	0.14	2.34	5.77	3.34	2.57	3.77	3.15	3.33	3.58	2.31	0.42	0.22	0.18
V	575	1045	1076	22	59	51	28	50	67	31	64	89	42	17	23
W	42	46	39	bdl	bdl	bdl	bdl	0.341	0.409	bdl	bdl	bdl	bdl	bdl	bdl
Y	9.18	9.24	14	16	27	23	12	20	25	29	41	31	1.67	0.63	1.35
Zn	87	86	113	42	86	64	24	65	76	22	113	196	165	85	83
Zr	14	20	25	185	288	194	135	313	316	159	267	445	2.37	bdl	1.71

TABLE S13: Bulk geochemical data of the studied samples from the DBTS. Trace elements reported in ppm.

	Site 3	Site 5	Site 3			Site 5	Site 4		Site 6							Site 7
Rock type	Ultramafic cumulate	Orthogneiss	Am-gneiss						Metatonalite				Chlorite-schist	Ultramafic cumulate		Blueschist
Sample	OL60	OL08	OL61	OL62	OL63	OL06	OL21A	OL21B	OL39	OL40	OL43	OL42A	OL42B	OL54	OL55	VP07
Trace elements (ppm)																
As	2.21	bdl	bdl	bdl	bdl	bdl	bdl	bdl	bdl	bdl	bdl	bdl	bdl	1.18	bdl	bdl
Ba	bdl	655	bdl	72	bdl	8.82	9.40	5.90	24	< L.D.	27	6.55	bdl	bdl	bdl	789
Be	0.22	2.30	1.49	1.09	1.16	0.77	1.20	1.33	0.91	0.61	0.94	0.29	0.19	0.58	0.06	3.57
Bi	0.10	0.08	0.11	0.11	0.26	0.06	0.26	0.16	bdl	0.13	0.08	0.16	0.08	0.15	bdl	0.19
Cd	0.02	0.04	0.06	0.04	0.08	0.04	bdl	0.05	0.05	0.03	0.02	0.08	0.08	0.06	bdl	0.43
Co	158	5.01	1.93	1.82	3.01	2.63	0.78	2.08	4.09	3.02	3.26	9.24	53	122	70	6.08
Cr	2084	5.09	5.88	4.92	7.22	5.02	4.27	5.49	11	8.82	6.44	14	43	3829	1560	44
Cs	0.34	0.59	bdl	0.20	bdl	bdl	bdl	bdl	0.33	0.07	0.02	0.07	0.09	0.14	0.26	1.99
Cu	51	bdl	3.37	9.10	13	3.80	7.12	6.43	11	11	3.97	30	8.16	119	14	18
Ga	5.93	20	17	14	21	15	13	16	20	15	15	22	27	4.77	1.86	24
Ge	0.83	1.22	0.92	0.92	1.34	0.55	0.46	1.20	1.12	0.40	0.59	0.75	0.70	1.01	0.75	2.25
Hf	0.08	4.76	4.02	3.23	7.59	3.99	1.60	4.01	11	4.75	3.36	17	7.19	0.09	0.06	9.84
In	bdl	bdl	bdl	bdl	0.06	bdl	bdl	bdl	0.04	bdl	bdl	0.03	0.04	bdl	bdl	0.09
Mo	bdl	bdl	0.80	bdl	bdl	1.81	0.81	0.80	bdl	0.82	bdl	bdl	bdl	bdl	bdl	1.46
Nb	0.09	9.35	7.74	6.35	9.95	11	17	9.08	9.89	5.71	6.85	17	16	0.22	0.43	18
Ni	1538	2.39	bdl	2.24	3.16	3.11	2.02	2.59	16	4.29	5.53	19	197	2310	764	16
Pb	1.21	5.95	9.61	12	20	1.44	1.70	13	3.11	0.77	2.33	1.18	bdl	3.34	0.67	44
Rb	0.43	61	0.16	14	0.45	0.43	0.26	0.29	2.12	0.46	1.86	0.55	0.38	0.25	0.56	103
Sc	6.21	4.96	6.61	4.53	17	6.84	1.33	4.72	6.37	4.36	3.41	8.92	9.42	8.99	4.08	23
Sb	0.28	0.17	0.16	0.11	0.24	0.23	0.15	0.22	bdl	bdl	bdl	bdl	bdl	0.35	0.12	bdl
Sn	bdl	1.42	3.00	2.14	2.18	2.81	2.59	2.69	6.76	3.25	2.62	7.31	6.19	0.34	0.36	2.84
Sr	4.56	226	326	212	797	39	37	350	69	9.84	85	32	8	1.82	0.70	363
Ta	0.01	0.85	0.86	0.70	1.00	1.24	6.94	0.68	0.41	0.30	0.68	0.81	0.81	0.02	0.03	1.46
Th	0.10	11	14	12	5.16	18	4.68	19	72	1.75	8.73	49	28	0.11	0.76	10
U	0.04	2.56	2.39	1.38	1.91	2.18	2.55	3.56	1.72	0.99	1.01	2.51	1.43	0.13	0.08	2.00
V	33	38	31	26	84	13	4.38	37	12	15	10	18	40	46	12	87
W	bdl	bdl	bdl	bdl	bdl	bdl	bdl	bdl	bdl	bdl	bdl	bdl	bdl	bdl	bdl	1.16
Y	1.86	14	17	13	22	18	3	12	19	6.81	14	18	13	2.06	0.73	51
Zn	102	58	30	24	62	14	7.32	30	33	21	19	31	172	129	105	140
Zr	2.17	174	133	109	327	124	41	147	326	201	121	541	254	2.02	1.73	404

TABLE S14: Bulk geochemical data of the studied samples from the DBTS. Trace elements reported in ppm.

	Site 1			Site 2											
Rock type	Hornblendite			Foliated orthogneiss	Mylonitic orthogneiss		Am-gneiss				Mu-rich layer	Chlorite-schist	Ultramafic cumulate		
Sample	OL02	OL03	OL04	OL25	OL24	OL23	OL50	OL68B	OL68A	OL49C	OL49B	OL49A	OL35	OL34	OL33
REE elements (ppm)															
La	1.89	3.19	4.07	59	45	43	30	36	30	40	45	39	1.37	1.21	0.76
Ce	5.39	8.55	12	119	94	86	60	72	60	82	93	80	3.95	2.64	2.01
Pr	0.92	1.27	1.99	12	10	8.90	6.15	8.10	7.18	8.79	10	8.97	0.64	0.30	0.37
Nd	5.14	6.01	10	41	37	31	21	29	27	32	38	35	2.86	1.10	1.66
Sm	1.67	1.72	3.09	6.28	6.43	5.48	3.52	4.81	5.38	6.28	8.04	7.08	0.56	0.18	0.44
Eu	0.63	0.57	0.82	0.99	1.58	1.22	0.93	1.68	1.48	1.33	2.20	1.76	0.07	0.02	0.07
Gd	1.77	1.72	2.96	4.29	5.19	4.56	2.71	3.80	4.66	5.31	7.21	6.11	0.39	0.12	0.30
Tb	0.30	0.28	0.50	0.59	0.79	0.69	0.38	0.57	0.73	0.83	1.17	0.93	0.05	0.02	0.04
Dy	1.90	1.76	3.02	3.20	4.71	4.20	2.20	3.41	4.48	5.10	7.27	5.78	0.25	0.09	0.22
Ho	0.38	0.35	0.59	0.62	0.97	0.87	0.46	0.71	0.94	1.05	1.51	1.17	0.06	0.02	0.04
Er	0.94	0.93	1.45	1.63	2.68	2.33	1.27	2.01	2.59	2.86	4.10	3.17	0.17	0.07	0.11
Tm	0.12	0.13	0.19	0.23	0.39	0.34	0.18	0.30	0.38	0.42	0.60	0.48	0.03	0.01	0.02
Yb	0.76	0.81	1.22	1.62	2.80	2.43	1.31	2.12	2.70	2.75	4.05	3.30	0.19	0.08	0.13
Lu	0.10	0.12	0.17	0.25	0.45	0.38	0.20	0.35	0.42	0.42	0.60	0.50	0.03	0.02	0.02
ΣREE	15	16	26	251	213	191	130	165	148	189	223	192	11	5.89	6.19

TABLE S15: Bulk geochemical data of the studied samples from the DBTS. Trace elements reported in ppm.

	Site 3	Site 5	Site 3			Site 5	Site 4		Site 6							Site 7
Rock type	Orthogneiss	Ultramafic cumulate	Amp-gneiss						Metatonalite				Chlorite-schist	Ultramafic cumulate		Blueschist
Sample	OL60	OL08	OL61	OL62	OL63	OL06	OL21A	OL21B	OL39	OL40	OL43	OL42A	OL42B	OL54	OL55	VP07
REE elements (ppm)																
La	0.53	49	30	27	22	32	9.11	49	102	7.76	21	86	40	1.41	1.03	43
Ce	1.13	97	61	54	47	68	18	95	234	16	47	188	91	2.67	3.68	96
Pr	0.16	9.67	6.65	5.75	5.42	7.38	1.97	9.42	28	1.81	5.31	22	10	0.28	0.46	12
Nd	0.64	32	23	20	22	26	6.54	30	101	6.82	19	78	36	1.04	1.90	48
Sm	0.18	4.85	4.31	3.56	4.60	4.90	1.26	4.58	23	1.47	4.21	16	7.98	0.25	0.48	11
Eu	0.06	1.10	0.87	0.73	1.48	0.71	0.21	0.84	1.11	0.76	0.91	1.32	0.83	0.10	0.03	1.69
Gd	0.19	3.52	3.49	2.80	4.15	3.88	0.91	3.28	15	1.31	3.29	10	5.56	0.29	0.33	10
Tb	0.04	0.47	0.51	0.40	0.64	0.58	0.13	0.42	1.54	0.19	0.48	1.12	0.67	0.05	0.04	1.52
Dy	0.27	2.70	3.12	2.44	4.03	3.50	0.67	2.29	6.08	1.13	2.64	4.79	3.10	0.36	0.18	9.34
Ho	0.06	0.51	0.63	0.49	0.84	0.70	0.13	0.44	0.80	0.25	0.51	0.72	0.51	0.08	0.03	1.95
Er	0.20	1.42	1.71	1.35	2.31	1.86	0.35	1.15	1.47	0.74	1.32	1.59	1.17	0.21	0.07	5.07
Tm	0.03	0.21	0.24	0.19	0.33	0.27	0.05	0.15	0.14	0.11	0.19	0.20	0.15	0.03	0.01	0.71
Yb	0.27	1.66	1.71	1.27	2.45	1.86	0.40	1.07	0.86	0.86	1.35	1.41	0.96	0.23	0.06	4.82
Lu	0.04	0.29	0.26	0.19	0.38	0.28	0.07	0.17	0.14	0.16	0.22	0.24	0.15	0.04	0.01	0.75
ΣREE	3.83	205	138	121	118	152	40	198	515	40	109	412	199	7	8	246

TABLE S16: Bulk geochemical data of the studied samples from the DBTS. Trace elements reported in ppm.

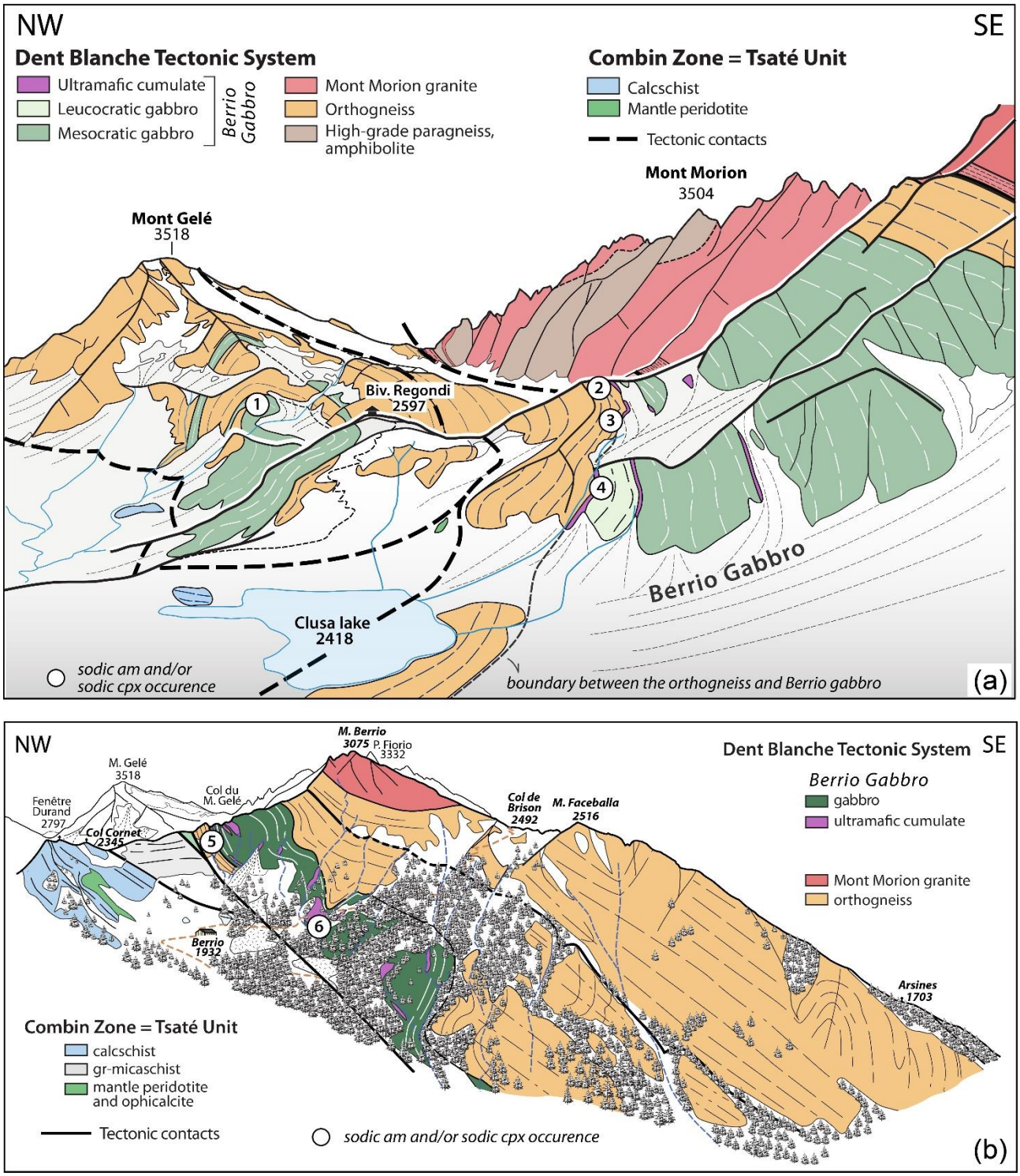

FIGURE S1 (a). Panorama of left bank of the Ollomont valley, between the Mont Gelé and the Mont Morion where sodic amphibole and sodic clinopyroxene (numbered white circles) have been found in the Dent Blanche Tectonic System. The Baseya Lake is located behind the small pass between the Regondi bivouac and site 2. (b) Panorama from Plan Debat, showing the contact between the Combin Zone (Tsaté Unit) and the Dent Blanche Tectonic System. The numbered white circles refer to the occurrences of sodic amphibole and/or sodic clinopyroxene in the Dent Blanche Tectonic System. Locality #7 (see Table 1) is not located in the area of the two panoramas. More details about the tectonic setting of the areas can be found in Manzotti *et al.*, 2017.

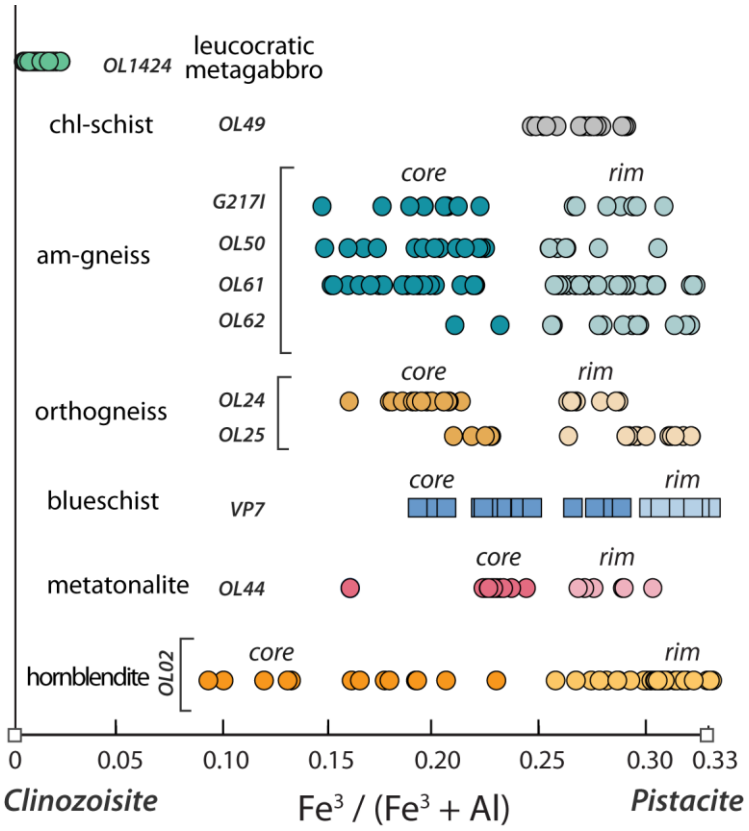

FIGURE S2: Chemical composition of epidote in the studied samples. Epidote in the leucocratic metagabbro (sample OL1424) shows the lowest Fe^{3+} content. In all the other samples, epidote displays an increase in Fe^{3+} from core to rim.

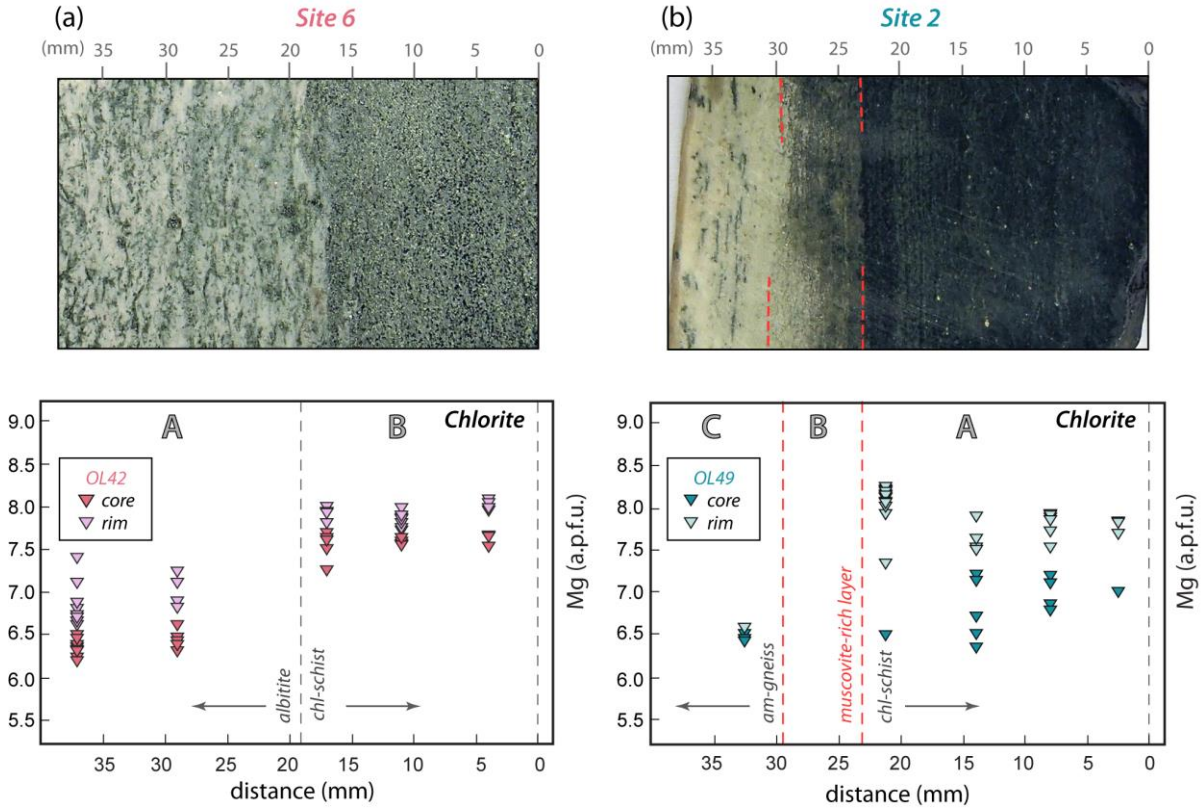

FIGURE S3 Photographs of the thin sections (sample OL42 and OL49) and chemical composition of chlorite at the contact with the ultramafic cumulate of the Berrio Gabbro (a) in the metatonalite (site 6) and (b) in the amphibole-gneiss and chlorite-schist along the profile of site 2.

P-H_2O modelling

The previous calculations are based on the assumption that H_2O was in excess during the metamorphic evolution. Here, we evaluate the possibility that metamorphism occurred under H_2O-undersaturated conditions. The aim of this modelling is to test if the absence of sodic amphibole in some rock types (e.g. in the orthogneiss and leucocratic metagabbro) can be linked to a limited H_2O content in the system. The red lines in the calculated *P*-H_2O pseudosections (Figs. S4 and S5) represent the H_2O–saturation surface and divide the diagrams in a H_2O-saturated (right) and a H_2O-undersaturated (left) part. All the calculated diagrams show that H_2O-undersaturation leads to important rapid variations of the stable mineral assemblages, including crystallisation of minerals commonly not expected for a given rock type. In the bulk compositions investigated, at a given *T*, the minimum *P* of the stability field of sodic amphibole is generally rapidly displaced to higher *P* with increasing H_2O-undersaturation.

A relatively large amount of H_2O (~ 4-4.5 wt%, depending on *P*; Fig. S4a) is required to reach H_2O-saturated conditions in the *hornblendite (OL02)*. With increasing H_2O-undersaturation, the minimum *P* of sodic amphibole stability first slightly decreases by ~0.5 kbar down to 8 kbar, then (for <3.4 wt% H_2O) rapidly increases up to >12kbar (for <1.3 wt% H_2O). When H_2O undersaturation is reached, the first changes of the mineral assemblages involve the disappearance of titanite, and the stabilisation of rutile, hornblende and garnet over the entire *P* interval explored. Chloritoid appears at $P > 8$ kbar, and staurolite for $P > 5.5$ kbar at H_2O ~1.6-2.6 wt%; kyanite becomes stable for H_2O contents lower than ~3 wt% at 12 kbar and ~1.8 wt% at 4 kbar. These minerals have never been observed in the studied sample. Consequently, the H_2O-saturated pseudosection yields the best match between the model and petrological observations.

A limited amount of H_2O (~ 0.2-0.3 wt%, depending of *P*; Fig. S4b) is required to reach H_2O-saturated conditions in the *metatonalite (OL43)*. The stability of sodic amphibole increases towards low *P* with incipient H_2O-undersaturation, with a minimum *P* of ~4.5 kbar for ~0.2 wt% H_2O. Lower H_2O contents lead however to a rapid increase of this minimum *P*. When H_2O undersaturation is reached, titanite is the first mineral that disappear from the stable assemblages, whereas hornblende, kyanite, cummingtonite, ilmenite, garnet and olivine become stable depending on *P* and the exact amount of H_2O. Again, the H_2O-saturated calculation provides the best fit between the model and petrological observations.

A relatively large amount of H_2O (~ 4-6.5 wt%, depending of *P*; Fig. S4c) is required to reach H_2O-saturated conditions in the *blueschist (VP7)*. Sodic amphibole is stable only at *P* higher than ~7 kbar and H_2O contents higher than ~3.5 wt% (H_2O saturation or limited undersaturation only). H_2O undersaturation leads to various modifications of the mineral assemblages (Fig. S4c). The most

important modification involve the stabilisation of biotite, hematite, K-feldspar and kyanite over the entire *P* interval studied. Yet, these minerals have never been observed in the studied rock.

A moderate H_2O amount of ~0.6-1.5 wt% (depending of *P*; Fig. S4d*)* is required to reach H_2O-saturated conditions in the *amphibole-gneiss (OL68B)*. Moderate H_2O-undersaturation increases the stability of sodic amphibole by ~1 kbar and ~2 kbar towards low and high *P*, respectively, but for low amounts of H_2O leads to its disappearance (Fig. S4d). When H_2O undesaturation is reached, titanite disappears at H_2O ~0.5-0.75 wt%. At lower H_2O content, hornblende, garnet, and kyanite, among others, become stable almost over the entire *P* interval explored. These minerals are never observed in the rock and consequently the assumption of H_2O in excess, which yields the best fit between observations and the thermodynamic modelling, appears as the most adapted.

The *leucocratic metagabbro (OL1424)* requires ~2.2-2.4 wt% of H_2O (depending of *P*; Fig. S5a) to reach H_2O-saturated conditions. Even moderate H_2O-undersaturation results in a rapid displacement of the minimum *P* limit of the stability field of sodic amphibole to higher *P*. From this point of view, H_2O-undersaturated conditions could explain the lack of sodic amphibole in this lithology. However, H_2O-undersaturation also leads to the appearance of minerals like hornblende, paragonite, kyanite, plagioclase, K-feldspar, or corundum (depending on *P* conditions), none of which was observed in this rock. The discrepancies between the petrological observations and the model indicate that the assumption of H_2O in excess for the modelling of the leucocratic metagabbro was correct.

As for the leucocratic metagabbro, in the *orthogneiss (14)* H_2O-undersaturation results in a rapid displacement of the minimum *P* limit of the stability field of sodic amphibole to higher *P* (Fig. S5b). Here again, however, minerals like garnet, kyanite and K-feldspar, never observed in the rock, become progressively stable with increasing H_2O-undersaturation. The discrepancies between petrological observations and the model suggest that the lack of free H_2O does not explain the absence of sodic amphibole in the orthogneiss.

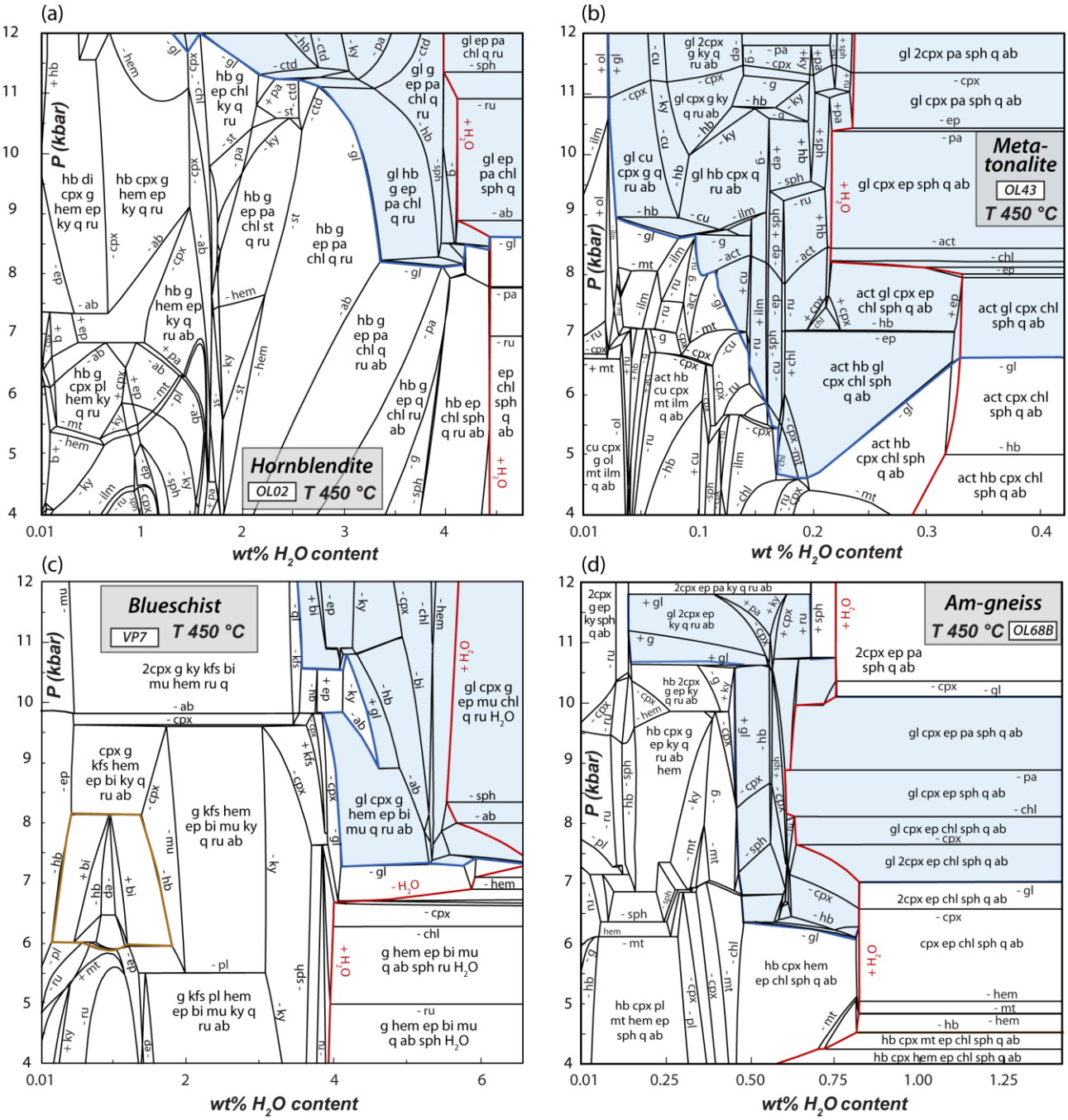

FIGURE S4 *P-X* H_2O pseudosections for the studied samples (a) OL02, hornblendite, (b) OL43, metatonalite (c) VP7, blueschist. The blue field indicates the *P-T* space where sodic amphibole is stable. Some fields are not labelled for sake of clarity; their mineral assemblages can be deduced from assemblages in adjacent fields. The red lines represent the H_2O-saturation surface and divide the diagram in a H_2O saturated (right) and in a H_2O-undersaturated (left) part.

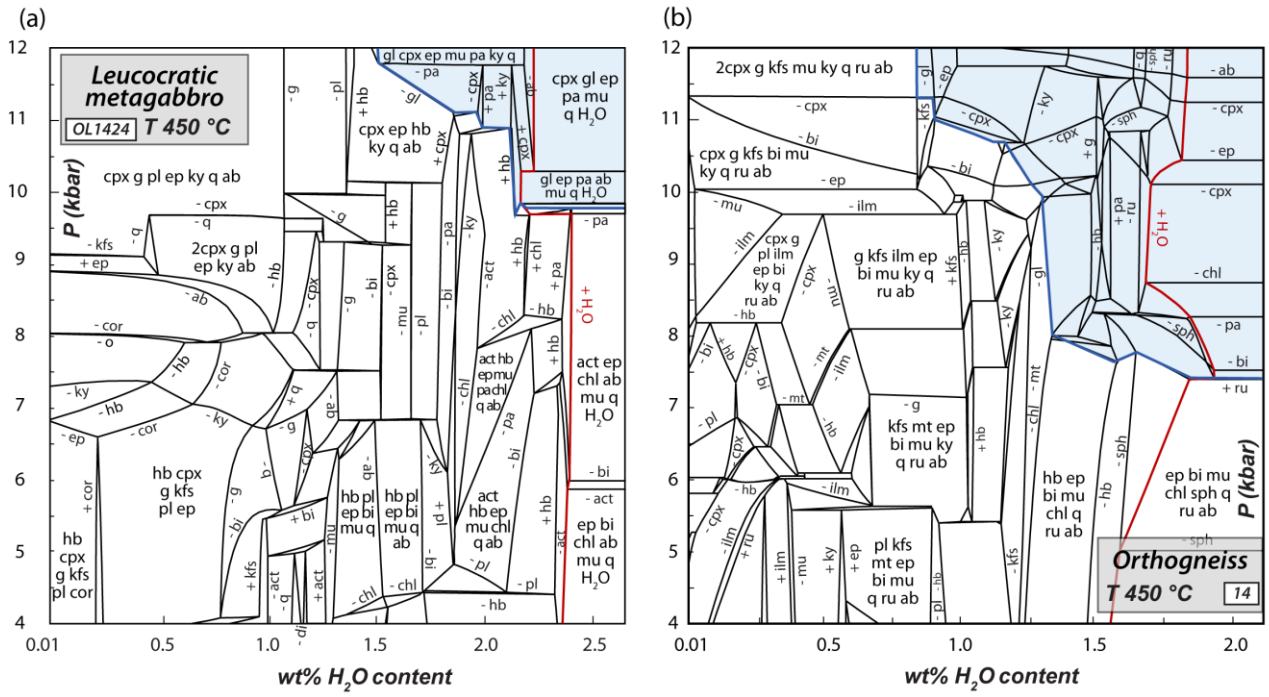

FIGURE S5 *P-X* H_2O pseudosections for the studied samples (a) OL1424, leucocratic metagabbro, (b) 14, orthogneiss. The blue field indicates the *P-T* space where sodic amphibole is stable. Some fields are not labelled for sake of clarity; their mineral assemblages can be deduced from assemblages in adjacent fields. The red lines represent the H_2O-saturation surface and divide the diagram in a H_2O saturated (right) and in a H_2O-undersaturated (left) part.

REFERENCES

Angiboust, S., Glodny, J., Oncken, O. & Chopin, C. (2014). In search of transient subduction interfaces in the Dent Blanche–Sesia Tectonic System (W. Alps). *Lithos* **205**, 298–321.

Ayrton, S., Bugnon, C., Haarpainter, T., Weidmann, M. & Frank, E. (1982). Géologie du front de la nappe de la Dent Blanche dans la région des Monts-Dolins, Valais. *Eclogae Geologicae Helvetiae* **75**, 269–286.

Baletti, L., Zanoni, D., Spalla, M. I. & Gosso, G. (2012). Structural and petrographic map of the Sassa gabbro complex (Dent Blanche nappe, Austroalpine tectonic system, Western Alps, Italy). *Journal of Maps* **8(4)**, 413–430.

Ballèvre, M. & Kienast, J.R. (1987). Découverte et signification de paragenèses a grenat amphibole bleue dans la couverture mésozoique de la nappe de la Dent-Blanche (Alpes Occidentales). *Comptes Rendus de l'Académie des Sciences Paris II* **305**, 43–46.

Canepa, A., Castelletto, M., Cesare, B., Martin, S. & Zaggia, L. (1990). The Austroalpine Mont Mary nappe (Italian Western Alps). *Memorie di Scienze Geologiche* **42**, 1-17.

Dal Piaz, G.V., Bistacchi, A., Gianotti, F., Monopoli, B. & Passeri, L. (2015). Note illustrative della Carta Geologica d'Italia alla scala 1:50000. *Servizio Geologico d'Italia, Roma*, *Foglio* **070** *Cervino,* 1-431.

De Leo, S., Biino, G. & Compagnoni, R. (1987). Riequilibrazioni metamorfiche alpine nella serie di Valpelline e di Arolla a Nord di Bionaz (Valpelline-Aosta). *Rendiconti della Società Italiana di Mineralogia e Petrologia* **42**, 181–182.

Diehl E. (1938). Geologisch-Petrographische Untersuchungen der Zone du Grand Combin im Val d'Ollomont. *Schweizerische Mineralogische und Petrographische Mitteilungen* **18**, 214-401.

Diehl, E. A., Masson, R. & Stutz, A. H. (1952). Contributo alla conoscenza del ricoprimento della Dent Blanche. *Memorie degli Istituti di Geologia e Mineralogia dell'Università di Padova* **17**,

1–52.

Stutz, A.H. (1940). Die Gesteine der Arollaserie im Valpelline (Provinz Aosta, Oberitalien). *Schweizerische mineralogische und petrographische Mitteilungen* **20**, 118-246.

Manzotti, P. (2011). Petro-structural map of the Dent Blanche tectonic system between Valpelline and Valtournenche valleys, Western Italian Alps—1: 20 000, 1: 10 000, 1: 2500. *Journal of Maps* **7**, 340–352.

Manzotti, P., Rubatto, D., Darling, J., Zucali, M., Cenki-Tok, B., Engi, M. (2012). From Permo-Triassic lithospheric thinning to Jurassic rifting at the Adriatic margin: petrological and geochronological record in Valtournenche (Western Italian Alps). *Lithos* **146-147**, 276-292.

Manzotti, P., Zucali, M., Ballèvre, M., Robyr, M., & Engi, M. (2014a). Geometry and kinematics of the Roisan-Cignana Shear Zone, and the orogenic evolution of the Dent Blanche Tectonic Ssytem (Western Alps). *Swiss Journal of Geosciences* **107**, 23-47.

Pennacchioni, G., & Guermani, A. (1993). The mylonites of the Austroalpine Dent Blanche nappe along the northwestern side of the Valpelline Valley (Italian Western Alps). *Memorie di Scienze Geologiche* **45**, 37-55.

Roda, M., & Zucali, M. (2008). Meso and microstructural evolution of the Mont Morion metaintrusives complex (Dent Blanche nappe, Austroalpine domain, Valpelline, Western Italian Alps). *Italian Journal of Geosciences* **127**, 105–123.

Roda, M., & Zucali, M. (2011). Tectono-metamorphic map of the Mont Morion Permian metaintrusives (Mont Morion-Mont Collon-Matterhorn Complex, Dent Blanche Unit), Valpelline-Western Italian Alps-1:10 000. *Journal of Maps* **7**, 519–535.